

CHAPTER 3 TUNED LIQUID COLUMN DAMPERS

There is nothing more practical than a good theory
- T. Von Karman

In this chapter, tuned liquid column dampers (TLCDs) are discussed. First, the mathematical model of the TLCD is presented and the equivalent linearized model is compared with the nonlinear model. Next, numerical optimization studies are conducted to determine the important parameters for optimum TLCD performance, namely, the tuning ratio and the damping ratio. In a later section, similar values of optimal parameters have been determined for multiple tuned liquid column dampers (MTLCDs).

3.1 Introduction

In the classical work on the Dynamic Vibration Absorber (also known as TMD), Den Hartog (1956) derived expressions for the optimum damping ratio and tuning ratio (i.e., ratio of the absorber frequency to the natural frequency of the primary system) for a coupled SDOF-TMD system subjected to harmonic excitation. The optimum absorber parameters which minimize the displacement response of the primary system were found to be simple functions of the mass ratio (ratio of mass of structure and damper). McNamara (1977) reported design of TMDs for buildings with attention to experimental studies and design considerations. Ioi and Ikeda (1978) developed empirical expressions to determine correction factors for optimum parameters in the case of lightly damped structures. Randall *et al.* (1981) and Warburton and Ayorinde (1980) further tabulated and

developed design charts for the optimum parameters for specified mass ratios and different primary system damping.

Previous work has been done with the aim of deriving optimum parameters for TLCDs. Abe *et al.* (1996) derived optimum parameters using perturbation techniques. Gao *et al.* (1997) studied numerically the optimization of TLCDs for sinusoidal excitations. Chang and Hsu (1998) have also discussed optimal absorber parameters for TLCDs for undamped structure attached to a TLCD. These dampers were found to be effective for wind loading (Xu *et al.* 1992; Balendra *et al.* 1995) and earthquake loading (Won *et al.* 1996; Sadek *et al.* 1998).

In this chapter, similar expressions have been developed and parameters have been tabulated for undamped and damped primary systems equipped with TLCDs. Usually, in the design of TMDs for wind and earthquake excitations, the optimum parameters are chosen to be those obtained by assuming a white noise random excitation. In this study, in addition to the white noise excitation, a set of filtered white noise (FWN) excitation has been considered for evaluating the optimal absorber parameters.

Optimum parameter analysis of MTLCDs is similar to MMDs (multiple mass dampers), where the important design parameters are the frequency range of the dampers and the damping ratio of the dampers (Yamaguchi and Harnpornchai, 1993; Kareem and Kline, 1995). MTLCDs are useful because the efficiency is higher as compared to a single TLCD and moreover, the sensitivity to the tuning ratio is diminished. Multiple liquid dampers have also been studied by Fujino and Sun (1993); Sadek *et al.* (1998) and Gao *et al.* (1999).

3.2 Modeling of Tuned Liquid Column Dampers

Figure 3.1 shows the schematic of the TLCD mounted on a structure represented as a SDOF system.

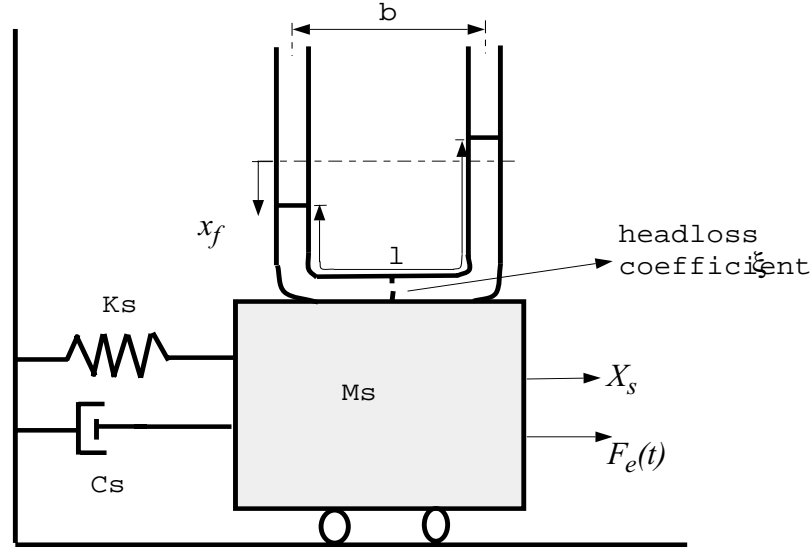


Figure 3.1 Schematic of the Structure-TLCD system

The equation describing the motion of the fluid in the tube is given as (Sakai *et al.* 1989),

$$\rho A l \ddot{x}_f(t) + \frac{1}{2} \rho A \xi |\dot{x}_f(t)| \dot{x}_f(t) + 2 \rho A g x_f(t) = -\rho A b \ddot{X}_s(t) \quad (3.1)$$

where the natural frequency of oscillations in the tube are given by $\omega_f = \sqrt{\frac{2g}{l}}$. The equa-

tion of motion for the primary system (structure) is given as,

$$(M_s + \rho A l) \ddot{X}_s(t) + \rho A b \ddot{x}_f(t) + C_s \dot{X}_s(t) + K_s X_s(t) = F_e(t) \quad (3.2)$$

where X_s = response of the primary system (structure); x_f = response of the liquid damper (TLCD); M_s = mass of the primary system; K_s = stiffness of the primary system; C_s = damping in the primary system = $2 M_s \zeta_s \omega_s$; ζ_s = damping ratio of the primary system; ω_s = natural frequency of the primary system; ρ = liquid density; A = cross sectional area

of the tube; l = total length of the liquid column; b = horizontal length of the column; g = gravitational constant; ξ = coefficient of headloss of the orifice. The two equations can be combined into the following matrix equation:

$$\begin{bmatrix} M_s + m_f & \alpha m_f \\ \alpha m_f & m_f \end{bmatrix} \begin{bmatrix} \ddot{X}_s \\ \ddot{x}_f \end{bmatrix} + \begin{bmatrix} C_s & 0 \\ 0 & c_f \end{bmatrix} \begin{bmatrix} \dot{X}_s \\ \dot{x}_f \end{bmatrix} + \begin{bmatrix} K_s & 0 \\ 0 & k_f \end{bmatrix} \begin{bmatrix} X_s \\ x_f \end{bmatrix} = \begin{bmatrix} F_e(t) \\ 0 \end{bmatrix}, |x_f| \leq \frac{(l-b)}{2}, \quad (3.3)$$

where α = length ratio = b/l ; m_f = mass of fluid in the tube = ρAl ; c_f = equivalent damping of the liquid damper = $2m_f\omega_f\zeta_f$; ζ_f = damping ratio of TLCD; ω_f = natural frequency of the liquid damper; k_f is the stiffness of the liquid column = $2\rho Ag$, and $F_e(t)$ is the external excitation. The constraint on Eq. 3.3 is placed so as to ensure that the liquid in the tube maintains the U-shape and the water does not spill out of the tube, thereby decreasing the dampers effectiveness.

3.2.1 Equivalent Linearization

Using the expressions derived in section 2.4, one can obtain equivalent linear damping for the nonlinear TLCD damping (c_f). In particular, using Eq. 2.20 one can obtain:

$$c_f = \frac{4\rho A\xi A_e\omega_e}{3\pi} \quad (3.4)$$

where the excitation force is harmonic, $F_e(t) = m_f A_e \omega_e^2 \sin(\omega_e t)$, while for random excitation, using Eq. 2.24:

$$c_f = \sqrt{\frac{2}{\pi}} \rho A \xi \sigma_{\dot{x}_f} \quad (3.5)$$

where $\sigma_{\dot{x}_f}$ is the standard deviation of the liquid velocity. This analytical model will be used in the rest of the study.

3.2.2 Accuracy of Equivalent linearization

Since the equivalent damping will be used in later studies on TLCs, it is useful to study the accuracy of the equivalent linearization method. The two equations, written in non-dimensional form, are as follows,

Nonlinear System:

$$\begin{bmatrix} 1 + \mu & \alpha\mu \\ \alpha & 1 \end{bmatrix} \begin{bmatrix} \ddot{X}_s \\ \ddot{x}_f \end{bmatrix} + \begin{bmatrix} 2\omega_s \zeta_s & 0 \\ 0 & \frac{\xi |\dot{x}_f|}{2l} \end{bmatrix} \begin{bmatrix} \dot{X}_s \\ \dot{x}_f \end{bmatrix} + \begin{bmatrix} \omega_s^2 & 0 \\ 0 & \omega_f^2 \end{bmatrix} \begin{bmatrix} X_s \\ x_f \end{bmatrix} = \begin{bmatrix} \frac{F_e(t)}{M_s} \\ 0 \end{bmatrix} \quad (3.6)$$

Equivalent Linear System:

$$\begin{bmatrix} 1 + \mu & \alpha\mu \\ \alpha & 1 \end{bmatrix} \begin{bmatrix} \ddot{X}_s \\ \ddot{x}_f \end{bmatrix} + \begin{bmatrix} 2\omega_s \zeta_s & 0 \\ 0 & 2\omega_f \zeta_f \end{bmatrix} \begin{bmatrix} \dot{X}_s \\ \dot{x}_f \end{bmatrix} + \begin{bmatrix} \omega_s^2 & 0 \\ 0 & \omega_f^2 \end{bmatrix} \begin{bmatrix} X_s \\ x_f \end{bmatrix} = \begin{bmatrix} \frac{F_e(t)}{M_s} \\ 0 \end{bmatrix} \quad (3.7)$$

where μ is the mass ratio = m_f/M_s . The nonlinear equations were simulated using the nonlinear differential equation solver in MATLABTM, while for the linear equation, an iterative method was used to solve the equivalent linearized equations. In the second case, one first assumes a value for $\sigma_{\dot{x}_f}$, simulates the linear system, recalculates the value of $\sigma_{\dot{x}_f}$ and iterates till the response quantity converges to an acceptable value. In this study, the main focus is to examine the error between the exact nonlinear and linearized equation for variations in the parameter ξ . The excitation used is a band-limited Gaussian white noise with a pulse width of 0.002 seconds and a spectral intensity of $0.01 \text{ m}^2/\text{sec}^3/\text{Hz}$.

Figure 3.2 shows the comparison of the response of the structure and damper for various headloss coefficients. The maximum error between the nonlinear and the equivalent linear system is about 2%. Figure 3.3 shows the time histories of the various response quantities for $\xi = 75$.

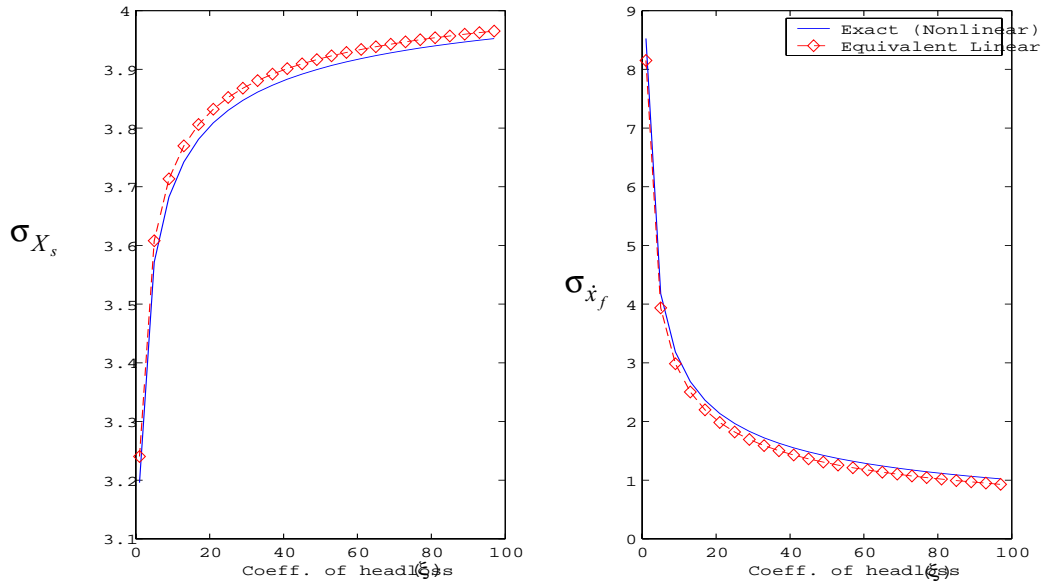


Figure 3.2 Exact (Non-linear) and Equivalent Linearization results

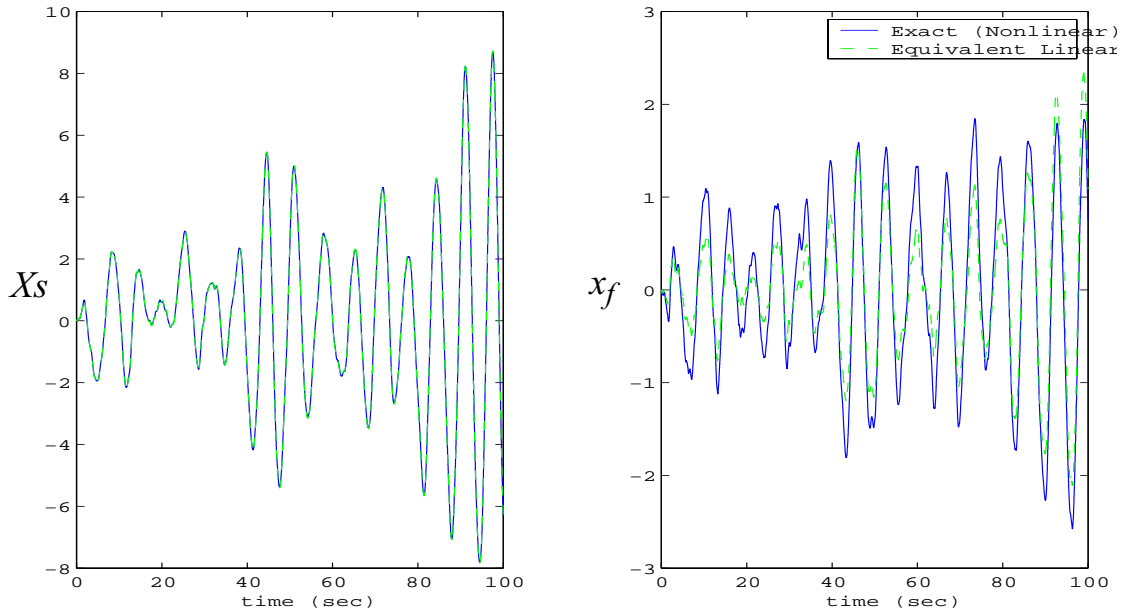


Figure 3.3 Time histories for $\xi = 75$

3.3 Optimum Absorber Parameters

It has been observed from numerical studies that the headloss coefficient affects the structure's frequency response curve. As the head-loss coefficient (ξ) increases, the response curve changes from a double hump curve to a single hump curve (Fig. 3.4). Numerical studies conducted by the author indicate that an optimal damping level exists for the TLCD which depends on the excitation level and the head loss coefficient. The first task, however, is to obtain the optimum damping ratio and tuning ratio of the absorber.

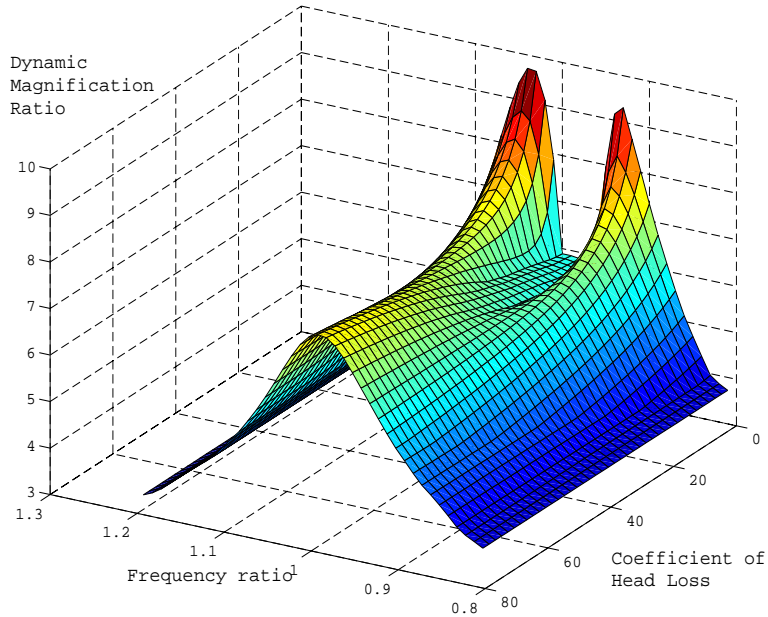


Figure 3.4 Variation of dynamic magnification factor with the head-loss coefficient and frequency ratio for a TLCD

The analytical model was discussed in section 3.2. One can define transfer functions in the

Laplace domain, namely $H_{X_s F}(s) = \frac{X_s(s)}{F_e(s)}$ and $H_{x_f F}(s) = \frac{x_f(s)}{F_e(s)}$, where the following

expressions are obtained :

$$H_{X_s F}(\omega) = \frac{\Delta \mu \alpha \omega^2 - \omega^2 + 2\zeta_f \omega_f(i\omega) + \omega_f^2}{[-\omega^2(1 + \mu) + 2\zeta_s \omega_s(i\omega) + \omega_s^2][-\omega^2 + 2\zeta_f \omega_f(i\omega) + \omega_f^2] + \omega^4 \alpha^2 \mu} \quad \text{and}$$

$$H_{x_f F}(\omega) = \frac{\alpha \omega^2 + \Delta}{[-\omega^2(1 + \mu) + 2\zeta_s \omega_s(i\omega) + \omega_s^2][-\omega^2 + 2\zeta_f \omega_f(i\omega) + \omega_f^2] + \omega^4 \alpha^2 \mu}$$

where $\Delta = 1$ for base excitation in which case X_s is the relative displacement, and $\Delta = 0$ for primary system excitation where X_s corresponds to the absolute displacement. One can compute the response quantities of interest using random vibration analysis. In particular, we are interested in the variance of the primary system displacement and the variance of the liquid velocity in the TLCD. The response quantities are obtained as,

$$\sigma_{X_s}^2 = \int_{-\infty}^{\infty} |H_{X_s F}(\omega)|^2 S_{FF}(\omega) d\omega \quad (3.8)$$

$$\sigma_{\dot{x}_f}^2 = \int_{-\infty}^{\infty} \omega^2 |H_{x_f F}(\omega)|^2 S_{FF}(\omega) d\omega \quad (3.9)$$

where $S_{FF}(\omega)$ is the power spectral density of the forcing function. Equation 3.9 is useful in evaluating the equivalent damping of the TLCD from Eq. 3.5. A simplified solution to the integral for random vibration analysis has been used to evaluate Eqs. 3.8 and 3.9 (see Appendix A.1 for details). Three representative forcing functions have been studied here, as listed in Table 3.1. The optimal absorber parameters are derived for each individual case of white noise and FWN excitations. It will be shown in subsequent sections that typical wind and earthquake excitations can be approximated through the use of such filters.

TABLE 3.1 Example forcing functions

Type of Excitation	$S_{FF}(\omega)$ Spectrum	Type of excitation
White Noise Excitation	S_0	primary system excitation
First Order Filter (FOF)	$\frac{S_0}{v_1^2 + \omega^2}$	primary system excitation
Second Order Filter (SOF)	$\frac{S_0\{c_1^2\omega^2 + d_1^2\}}{\left\{[b_1^2 - \omega^2]^2 + a_1^2\omega^2\right\}}$	primary system excitation and/or base excitation

Based on these three excitation models, optimal parameters have been obtained for TLCD attached to damped and undamped primary systems. It has been seen that one can derive an explicit expression for the case of undamped structure-TLCD system subjected to white noise. However, for damped systems and/or other excitations, the development of closed-form solutions is challenging. This is because some characteristics of the classical damper system, like invariance points, do not exist when damping is introduced in the primary system (Den Hartog, 1956). Therefore, the optimal absorber parameters (i.e., ζ_f and $\gamma = \omega_f/\omega_s$) are obtained numerically for these cases. The optimal conditions are obtained by setting:

$$\frac{\partial \sigma_{x_s}^2}{\partial \zeta_f} = 0 ; \quad \frac{\partial \sigma_{x_s}^2}{\partial \gamma} = 0 \quad (3.10)$$

One can obtain ζ_{opt} and γ_{opt} by solving the two conditions given by Eq. 3.10

In the case of tuned mass dampers, a detailed analysis was carried out by Warburton (1982) to determine optimum damper parameters for the case of random excitations (represented by white noise), with excitation applied to the structure (as in the case of

wind) or as a base acceleration (as in the case of ground motion). The design of TMDs for wind and earthquake applications, therefore, uses these design expressions for the optimal parameters. In the next sub-sections, the theory to determine the optimal parameters is presented for the example forcing functions listed in Table 3.1.

3.3.1 White Noise excitation

The response integral in Eqs. 3.8 and 3.9 can be cast in the following form:

$$\sigma_{x_s}^2 = S_0 \int_{-\infty}^{\infty} \frac{\Xi_n(\omega) d\omega}{\Lambda_n(-i\omega)\Lambda_n(i\omega)} \quad (3.11)$$

Details of the integration scheme can be found in Appendix A.1.

Undamped Primary System

Solving the two optimization conditions in Eq. 3.10 and setting $\zeta_s = 0$ yields:

$$\zeta_{opt} = \frac{\alpha}{2} \sqrt{\frac{\mu \left(1 + \mu - \alpha^2 \frac{\mu}{4}\right)}{(1 + \mu) \left(1 + \mu - \frac{\alpha^2 \mu}{2}\right)}}; \quad \gamma_{opt} = \frac{\sqrt{1 + \mu \left(1 - \frac{\alpha^2}{2}\right)}}{1 + \mu} \quad (3.12)$$

In case, one can assume the tuning ratio to be equal to one, one can obtain a simpler expression for the optimal damping given by,

$$\zeta_{opt} = \frac{1}{2} \sqrt{\frac{\mu(\mu + \alpha^2)}{(1 + \mu)}} \quad (3.13)$$

This is justifiable because for the low mass ratios of the order 1-2% practical for tall buildings, the tuning ratio is close to one, and in this case the optimal damping coefficient given by Eq. 3.13 approximates Eq. 3.12 quite well. Similar expressions exist for an optimal damping coefficient and tuning ratio of a TMD given by Warburton and Ayorinde (1980),

$$\zeta_{opt} = \frac{1}{2} \sqrt{\frac{\mu \left(1 + \frac{3\mu}{4}\right)}{(1 + \mu) \left(1 + \frac{\mu}{2}\right)}}; \quad \gamma_{opt} = \frac{\sqrt{1 + \frac{\mu}{2}}}{1 + \mu} \quad (3.14)$$

Note that in all cases considered, the optimum damping coefficient is independent of the value of S_0 , the intensity of white noise excitation. It is noteworthy that Eq. 3.14 reduces to Eq. 3.12 as α approaches 1. Comparison of optimal parameters under different optimization criteria are summarized in Table 3.2 for TMDs and TLCDs. Figure 3.5 shows the variation of optimum parameters as a function of the mass ratio. As the length ratio increases, the damping ratio increases because there is more mass in the horizontal portion of the TLCD. This contributes to indirect damping, which implies that it is better to keep the length ratio as high as possible without violating the constraints of the TLCD or the limitations of structural/architectural considerations.

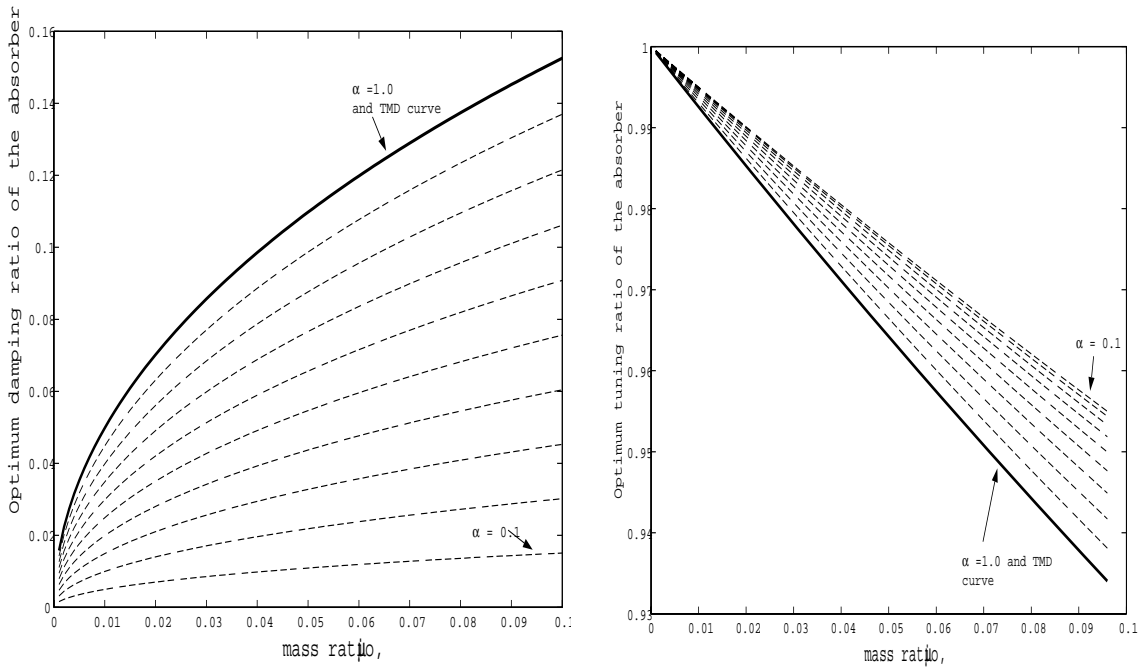


Figure 3.5 Comparison of optimum absorber parameters for a TLCD with varying α and a TMD.

TABLE 3.2 Comparison of optimal parameters for TMD and TLCD

Case number and parameter optimized			TMD		TLCD	
			γ_{opt}	ζ_{opt}	γ_{opt}	ζ_{opt}
1	Random Force acting on Structure	$\langle X_s^2 \rangle$	$\frac{\sqrt{1+\frac{\mu}{2}}}{1+\mu}$	$\frac{1}{2} \sqrt{\frac{\mu(1+\frac{3\mu}{4})}{(1+\mu)(1+\frac{\mu}{2})}}$	$\frac{\sqrt{1+\mu(1-\frac{\alpha^2}{2})}}{1+\mu}$	$\frac{\alpha}{2} \sqrt{\frac{\mu(1+\mu-\alpha^2\frac{\mu}{4})}{(1+\mu)(1+\mu-\frac{\alpha^2\mu}{2})}}$
2	Random acceleration at the base	$\langle X_s^2 \rangle$	$\frac{\sqrt{1-\frac{\mu}{2}}}{1+\mu}$	$\frac{1}{2} \sqrt{\frac{\mu(1-\frac{\mu}{4})}{(1+\mu)(1-\frac{\mu}{2})}}$	$\frac{\sqrt{1+\mu(1-\frac{3\alpha^2}{2})}}{1+\mu}$	$\frac{\alpha}{2} \sqrt{\frac{\mu(1-\mu+3\alpha^2\frac{\mu}{4})}{(1+\mu)(1+\mu-\frac{3\alpha^2\mu}{2})}}$
3	Random Force acting on Structure	$\langle \dot{X}_s^2 \rangle$	same as case 2	same as case 2	same as case 2	same as case 2
4	Random acceleration at the base	$\langle \dot{X}_s^2 \rangle$	same as case 1	same as case 1	same as case 1	same as case 1

Damped Primary System

As discussed earlier, it is not convenient to obtain a closed-form solution for optimum damper parameters for a damped primary system; therefore, it must be estimated numerically (Warburton, 1982). These computations have been conducted for $\zeta_s = 1, 2$ and 5% and $\mu = 0.5, 1, 1.5, 2$ and 5% and optimum absorber parameters are presented in Table 3.3.

Table 3.3 shows that as the mass ratio increases, ζ_{opt} also increases. Equation 3.12 verifies this for undamped case, since it is approximately proportional to the square root of the mass ratio. The tuning ratio also decreases as the mass ratio and the damping in the primary system increase, which is consistent with the results obtained for tuned mass

dampers. It is observed that for small values of ζ_s , ζ_{opt} is not affected; therefore for a lightly damped system, the optimum absorber parameters derived for an undamped primary system are valid. For higher levels of damping in the primary system, one can derive empirical expressions for the optimum damping ratio as a function of the primary system damping ratio.

TABLE 3.3 Optimum parameters for white noise excitation for different mass ratios.

	Undamped primary system		1% Damping		2% Damping		5% Damping	
	γ_{opt}	ζ_{opt}	γ_{opt}	ζ_{opt}	γ_{opt}	ζ_{opt}	γ_{opt}	ζ_{opt}
$\mu=0.5\%$	0.9965	0.0317	0.9962	0.0317	0.9958	0.0317	0.995	0.0317
$\mu=1\%$	0.993	0.0448	0.9925	0.0448	0.9921	0.0448	0.9908	0.0448
$\mu=1.5\%$	0.9896	0.0547	0.989	0.0547	0.9885	0.0547	0.9869	0.0547
$\mu=2\%$	0.986	0.0631	0.9855	0.0631	0.985	0.0631	0.983	0.0631
$\mu=5\%$	0.966	0.0986	0.965	0.0986	0.964	0.0986	0.962	0.0986

3.3.2 First order filter (FOF)

The forcing function for a FOF has a spectrum given by,

$$S_{FF}(\omega) = \frac{S_0}{v_1^2 + \omega^2} \quad (3.15)$$

This type of function can be used to approximate wind-induced positive pressures for the alongwind loading. Figure 3.6 (a) shows the transfer functions of the first order filter with different values of the parameter v_1 . Also shown for reference is the transfer function of the primary system. Table 3.4 gives the optimum absorber parameters for these first order filters. Note that when $v_1=10$, the optimum parameters are the same as those obtained for white noise, since the filter is fairly uniform like white noise excitation around the natural

frequency of the primary system. However, for other cases (e.g., $\nu_1 = 0.1$ and 1), the optimum parameters are slightly different. The effect is more pronounced in the case of the tuning ratio and increases as the damping in the primary system increases. Optimum parameters have been computed for $\nu_1 = 1$ and tabulated in Table 3.5. Though the optimal parameters can be obtained through the simultaneous solution of the two non-linear equations resulting from Eq. 3.10, the task becomes computationally intensive for the first and second order filters. In this numerical study, optimal parameters were obtained by utilizing the MATLAB optimization toolbox (Grace, 1992).

TABLE 3.4 Optimum absorber parameters for FOF for different parameter ν_1

parameter of first order filter	γ_{opt}	ζ_{opt}
$\nu_1 = 0.1$	0.991	0.04477
$\nu_1 = 1$	0.992	0.04476
$\nu_1 = 5$	0.9925	0.04483
$\nu_1 = 10$	0.993	0.04482

(These values are computed for undamped primary system with $\mu = 1\%$)

TABLE 3.5 Optimum absorber parameters for FOF for various mass ratios.

$\nu_1 = 1$	Undamped primary system		1% Damping		2% Damping		5% Damping	
	γ_{opt}	ζ_{opt}	γ_{opt}	ζ_{opt}	γ_{opt}	ζ_{opt}	γ_{opt}	ζ_{opt}
$\mu=0.5\%$	0.993	0.03197	0.992	0.03190	0.991	0.03185	0.988	0.0317
$\mu=1\%$	0.992	0.04476	0.991	0.04474	0.990	0.04470	0.987	0.04456
$\mu=1.5\%$	0.986	0.05484	0.985	0.05476	0.984	0.05468	0.979	0.0545
$\mu=2\%$	0.984	0.0630	0.983	0.0629	0.9815	0.06287	0.978	0.0626
$\mu=5\%$	0.962	0.0980	0.960	0.09795	0.958	0.0978	0.953	0.09727

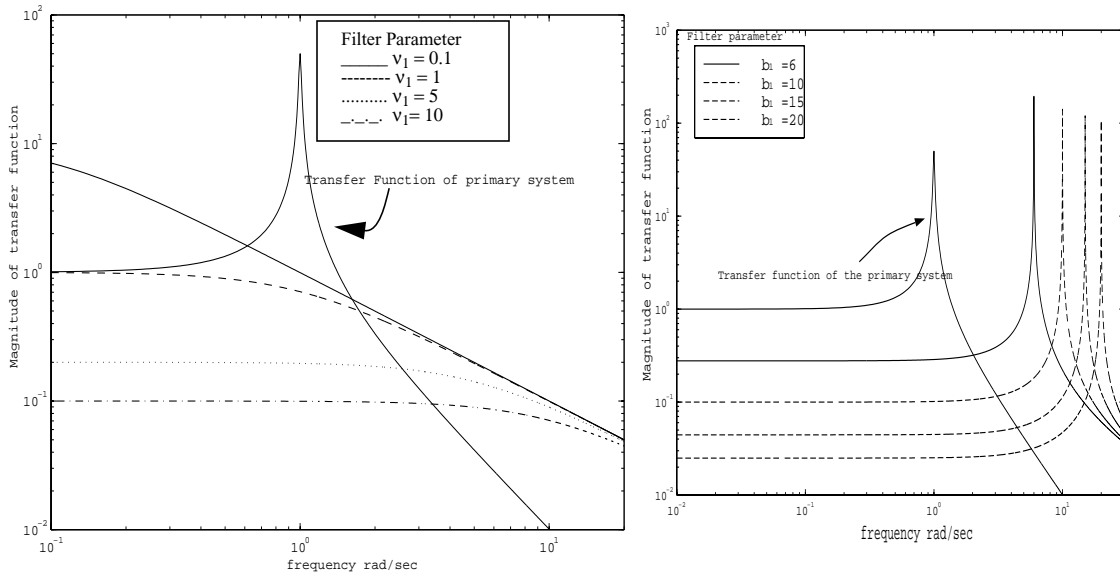


Figure 3.6 Transfer function of the filters and the primary system: (a) first order filters (b) second order filters

3.3.3 Second order filter (SOF)

A general second order filter studied here has the following spectral description,

$$S_{FF}(\omega) = \frac{S_0 \{c_1^2 \omega^2 + d_1^2\}}{\left\{ [b_1^2 - \omega^2]^2 + a_1^2 \omega^2 \right\}} \quad (3.16)$$

where a_1 , b_1 , c_1 and d_1 are the parameters of the filter. Second order filters can be used to represent earthquake and wind excitations. For earthquake representation, the excitation acts at the base of the structure, while for wind representation, the excitation acts on the structure. The expression in Eq. 3.16 also describes the well known Kanai-Tajimi spectrum (Kanai, 1961; Tajimi, 1960):

$$S_{FF}(\omega) = \frac{S_0 \left[1 + 4\zeta_g^2 \left(\frac{\omega}{\omega_g} \right)^2 \right]}{\left\{ \left[1 - \left(\frac{\omega}{\omega_g} \right)^2 \right]^2 + 4\zeta_g^2 \left(\frac{\omega}{\omega_g} \right)^2 \right\}} \quad (3.17)$$

where ω_g is the dominant ground frequency and ζ_g is the ground damping factor.

Similarly, the across-wind excitation can be modeled as a FWN using a second order filter. Kareem (1984) has proposed the following empirical expression for the spectral density of the across-wind force for square buildings:

$$\begin{aligned} \frac{nS_{FF}(z, n)}{\sigma_f^2} &= \alpha_o \beta_o \left(\frac{n}{n_s}\right)^\delta \text{ for } n \leq n_s \\ &= \alpha_o \beta_o \left(\frac{n}{n_s}\right)^{3.0} \text{ for } n \geq n_s \end{aligned} \quad (3.18)$$

$$\text{where } \alpha_o = \frac{\hat{b}}{\left[1 - \left(\frac{n}{n_s}\right)^2\right]^2 + \left[2b\left(\frac{n}{n_s}\right)\right]^2} \quad ; \quad \beta_o = 1.32 \left[\left(\frac{1}{3\tilde{\alpha}}\right)^{0.5} + 0.154 \left(1 - \frac{z}{H}\right)^{3.5} \right]; \quad n_s$$

is the shedding frequency $= \frac{S\bar{U}(z)}{B}$; B is the breadth of the building; $\bar{U}(z)$ is the mean speed at height z ; S is the Strouhal number; σ_{FF}^2 is the mean square value of the fluctuating across-wind force; $\tilde{\alpha}$ is the exponent term in the power law of the wind velocity profile; H is the height of the building; \hat{b} is the band width coefficient $= \sqrt{2}I(z)$, where $I(z)$ is the turbulence intensity at height z ; and $\delta = 0.9$. Details of this model can be found in Kareem (1984). This across-wind loading model can also be represented by Eq. 3.16.

The magnitude of the transfer function of the filter given by Eq. 3.16 is shown in Fig. 3.6 (b) for parameters $a_I = 0.01$, $c_I = 1$, $d_I = 10$ and varying $b_I = 6, 10, 15$ and 20 . Table 3.6 shows how the optimal parameters are influenced as the filter parameter b_I changes. As b_I increases, the assumption of purely white noise becomes valid and the solution approaches that for the white noise case. The other parameters have been kept the same and optimal parameters have been computed for damped and undamped cases (Table 3.7).

TABLE 3.6 Optimum absorber parameters for SOF for different values of b_I

parameter of SOF	γ_{opt}	ζ_{opt}
$b_I = 6$	1.05	0.1111
$b_I = 10$	1.01	0.0702
$b_I = 15$	1.00	0.0572
$b_I = 20$	0.995	0.0524

(All the other parameters are kept constant $a_I = 0.01$, $c_I = 1$, $d_I = 10$, $\mu = 0.02$ and $\zeta_s = 0.05$)

TABLE 3.7 Optimum absorber parameters for SOF for various mass ratios.

$a_I = 0.01$ $b_I = 36$ $c_I = 1$ $d_I = 10$	Undamped primary system		1% Damping		2% Damping		5% Damping	
	γ_{opt}	ζ_{opt}	γ_{opt}	ζ_{opt}	γ_{opt}	ζ_{opt}	γ_{opt}	ζ_{opt}
$\mu = 0.5\%$	1.04	0.1510	1.04	0.1401	1.045	0.1299	1.05	0.0956
$\mu = 1\%$	1.04	0.1559	1.04	0.1450	1.045	0.1350	1.05	0.1008
$\mu = 1.5\%$	1.04	0.1606	1.04	0.1498	1.045	0.1399	1.05	0.106
$\mu = 2\%$	1.04	0.1654	1.04	0.1546	1.045	0.1448	1.05	0.1111
$\mu = 5\%$	1.04	0.1927	1.04	0.1821	1.045	0.173	1.05	0.1406

As in previous cases, ζ_{opt} decreases as the damping in the primary system increases and increases as the mass ratio increases; however, the damping in the primary system affects ζ_{opt} more in this case than in the case of white noise. In addition, the tuning ratio slightly departs from $\gamma = 1.00$ as the damping in the primary system increases.

3.3.4 EXAMPLE

The optimum parameters for a TLCD placed on an eight story structure subjected to an earthquake excitation are determined in this example using the theory presented in the previous section. The parameters of the building stories considered are: floor mass = 345.6 tons, elastic stiffness = 34040 kN/m and internal damping coefficient = 2937 tons/sec, which corresponds to a 2% damping for each vibrational mode of the structure. The

computed natural frequencies are 5.79, 17.18, 27.98, 37.82, 46.38, 53.36, 58.53 and 61.69 rad/sec. The base excitation is modeled by the Kanai-Tajimi spectrum given in Eq. 3.17 with the parameters $\omega_g = 10.5$ rad/sec and $\zeta_g = 0.317$. The parameters of the general second order filter can be related to these as follows: $a = c = 2\zeta_g$ and $b = d = \omega_g$. The mass of the damper has been taken as 2% of the first generalized mass of the structure. In Table 3.8, the optimum design damper parameters for the TMD have been compared with TLCD parameters, both under the white noise and the SOF excitations. It is noted that there are significant differences in the optimum absorber parameters, justifying the inclusion of the anticipated loading in the optimization process for the damper design.

TABLE 3.8 Optimum absorber parameters

	TMD	TLCD (white noise)	TLCD (SOF)
γ_{opt}	0.98	0.985	1.027
ζ_{opt}	7.3 %	6.31 %	6.51 %

3.4 Multiple tuned liquid column dampers (MTLCDs)

Multiple units of TLCDs can be incorporated in a structural system at one location or distributed spatially. In this system, the natural frequencies of the TLCDs are distributed over a range of frequencies. The advantages of a distributed system is that it is more robust and effective for excitation frequencies distributed over a wide frequency band. In the following study, MTLCD configuration design parameters are evaluated.

The primary system is represented as a single degree of freedom (SDOF) system and the secondary system, in this case, is the system of MTLCDs. The equations of motion of the SDOF-MTLCD system (Fig. 3.7) can be written in a matrix notation as:

$$\begin{bmatrix} \tilde{m}_s & \mathbf{m}_f^T \\ \mathbf{m}_f & \mathbf{m} \end{bmatrix} \begin{bmatrix} \ddot{X}_s \\ \dot{\mathbf{x}}_{fn} \end{bmatrix} + \begin{bmatrix} C_s & \mathbf{0} \\ \mathbf{0} & \mathbf{c}_{eqn} \end{bmatrix} \begin{bmatrix} \dot{X}_s \\ \dot{\mathbf{x}}_{fn} \end{bmatrix} + \begin{bmatrix} K_s & \mathbf{0} \\ \mathbf{0} & \mathbf{k}_{eqn} \end{bmatrix} \begin{bmatrix} X_s \\ \mathbf{x}_{fn} \end{bmatrix} = \begin{bmatrix} F_e(t) \\ \mathbf{0} \end{bmatrix} \quad (3.19)$$

where $\tilde{m}_s = M_s + \sum_{n=1}^N m_{fn}$; $\mathbf{m}_f^T = \alpha [m_{f1} \ m_{f2} \ \dots \ m_{fN}]$;

$$\mathbf{m} = \begin{bmatrix} m_{f1} & 0 & 0 & 0 \\ 0 & m_{f2} & 0 & 0 \\ 0 & 0 & \dots & \dots \\ 0 & 0 & \dots & m_{fN} \end{bmatrix} ; \mathbf{c}_{eqn} \text{ and } \mathbf{k}_{eqn} \text{ are } (n, n) \text{ diagonal matrices similar to } \mathbf{m} .$$

The transfer function of the primary system is obtained by non-dimensionalising Eq. 3.19,

$$H_{X_s F}(\omega) = \frac{1}{\left[-\omega^2 \left(1 + \sum_{n=1}^N \mu_{fn} \right) + 2\zeta_s \omega_s (i\omega) + \omega_s^2 \right] + \alpha^2 \omega^4 \sum_{n=1}^N \frac{\mu_{fn}}{[-\omega^2 + 2\zeta_{fn} \omega_{fn} (i\omega) + \omega_{fn}^2]}}$$

and the transfer function for each TLCD is given by,

$$H_{x_{fn} F}(\omega) = \frac{\alpha i \omega^2 H_{X_s F}(\omega)}{[-\omega^2 + 2\zeta_{fn} \omega_{fn} (i\omega) + \omega_{fn}^2]} ; n=1..N$$

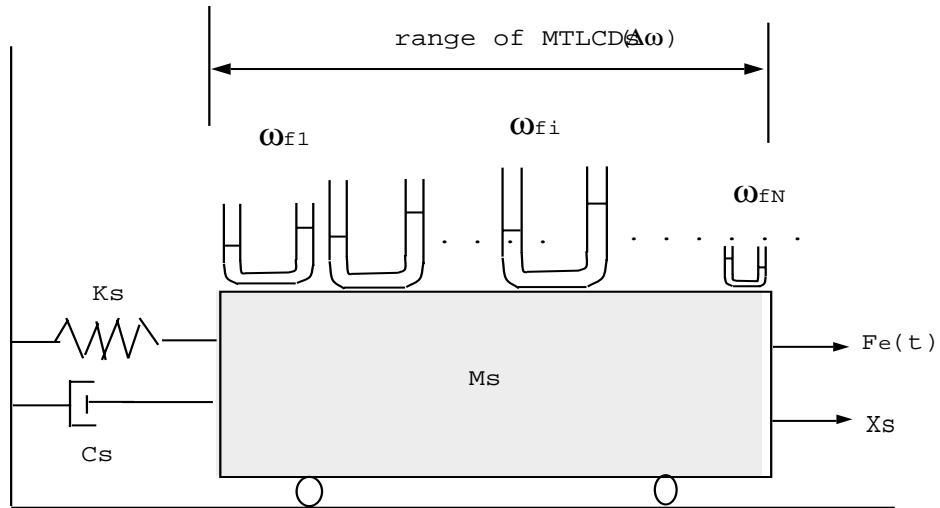


Figure 3.7 MTLCD configuration

The analysis of MTLCDs is similar to MMDs (multiple mass dampers), where the important design parameters are the frequency range and damping ratio of the dampers (Kareem and Kline, 1995). The frequency range is defined as the total frequency span of

the MTLCDs given as $\Delta\omega = \omega_{fN} - \omega_{f1}$. The central damper ($n = (N+1)/2$) is tuned exactly to the natural frequency of the primary system. It is assumed that N is an odd number in this analysis. The frequency of each damper can be written as,

$$\begin{aligned}\omega_{fn} &= \omega_s - \frac{\Delta\omega}{N}n ; \quad 1 \leq n < \frac{N+1}{2} \\ &= \omega_s \quad ; \quad n = \frac{N+1}{2} \\ &= \omega_s + \frac{\Delta\omega}{N}n ; \quad N \geq n > \frac{N+1}{2}\end{aligned}$$

A numerical study has been conducted to examine the effects of the number of dampers, frequency range and damping ratio of the dampers. Optimum values of these parameters have been obtained by minimization of the RMS displacement.

3.4.1 Effect of number of dampers (N)

From Fig. 3.8, one can observe the flattening action of MTLCDs as compared to the double peaked response due to an STLCD. The effect of increasing dampers is similar to that of adding damping: i.e., flattening of the frequency response function. However, it is also noted that the frequency response due to 5, 11 and 21 TLCD groups, for the particular frequency range of 0.2, are very similar. This suggests that a large number of TLCDs do not necessarily mean better performance, limiting the advantage of utilizing large number of MTLCDs for a particular frequency range.

3.4.2 Effect of damping ratio of dampers (ζ_{fn})

The damping ratio of MTLCDs is studied for a group of eleven dampers with a fixed frequency range of 0.2 (Fig. 3.9). It is noted that at low damping ratios, the amplitude of the response function is spiked. As the damping ratio is increased, the response

function slowly becomes smoother and the amplitude decreases. After an optimal damping ratio for the dampers is reached, any further increase in the damping ratio results in an increase in the amplitude. This suggests that there exists an optimum damping ratio for a particular set of MTLCD configurations.

3.4.3 Effect of frequency range ($\Delta\omega$)

Figure 3.10 shows the effect of changing the frequency range on the frequency response function. It can be seen from the plots that there is an optimum range where the curve flattens out over a range of frequencies. The frequency response functions of an STLCD and a MTLCD with a low frequency range (0.02 and smaller) are similar. If the range is smaller than the optimum, the frequency response of the MTLCD resembles that of an STLCD, and so in a way, the MTLCD loses its effectiveness. This is intuitive because there is a practical limit to which one can distribute the MTLCDs over a given frequency range. As this range becomes very small, MTLCDs act almost like an STLCD.

Two types of configurations can be considered for multiple TLCDs: SDOF-MTLCD configuration (to control single mode of the structure) and MDOF-MTLCD configuration (to control multiple modes). The time frequency analysis of several earthquake ground motion records utilizing wavelets has revealed the presence of higher frequency components in the initial stages of the event, e.g., El-Centro (Gurley and Kareem, 1994). In such cases, the presence of a TLCD or MTLCD tuned to the higher modes will be essential in controlling motion induced by higher frequency components.

Table 3.9 tabulates the optimum parameters of the different MTLCD system. One can note that the optimum damping ratio decreases drastically for MTLCD groups as compared to an STLCD.

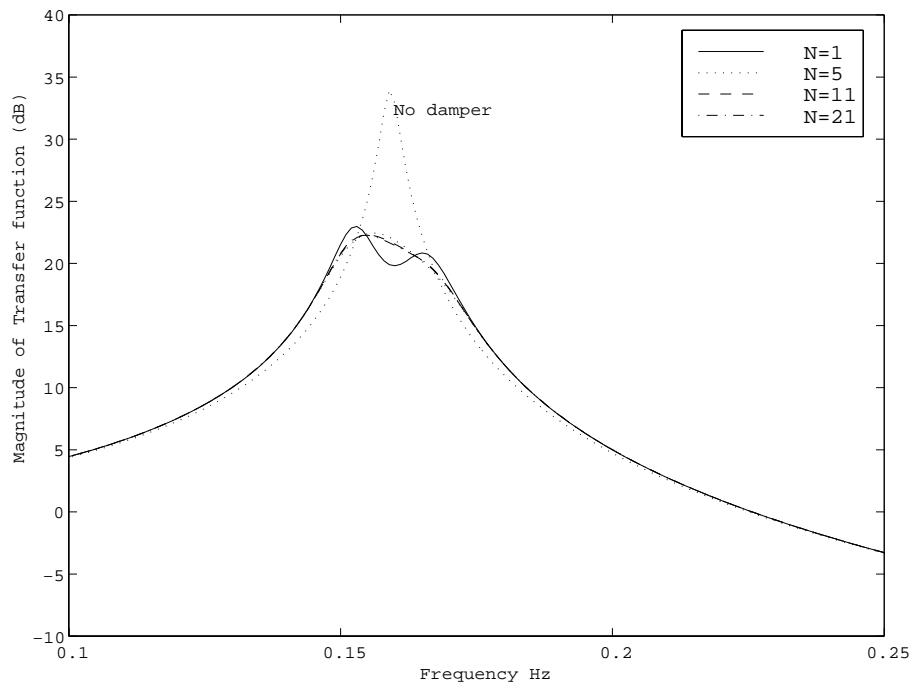


Figure 3.8 Effect of number of dampers on the frequency response of SDOF-MTLCD system

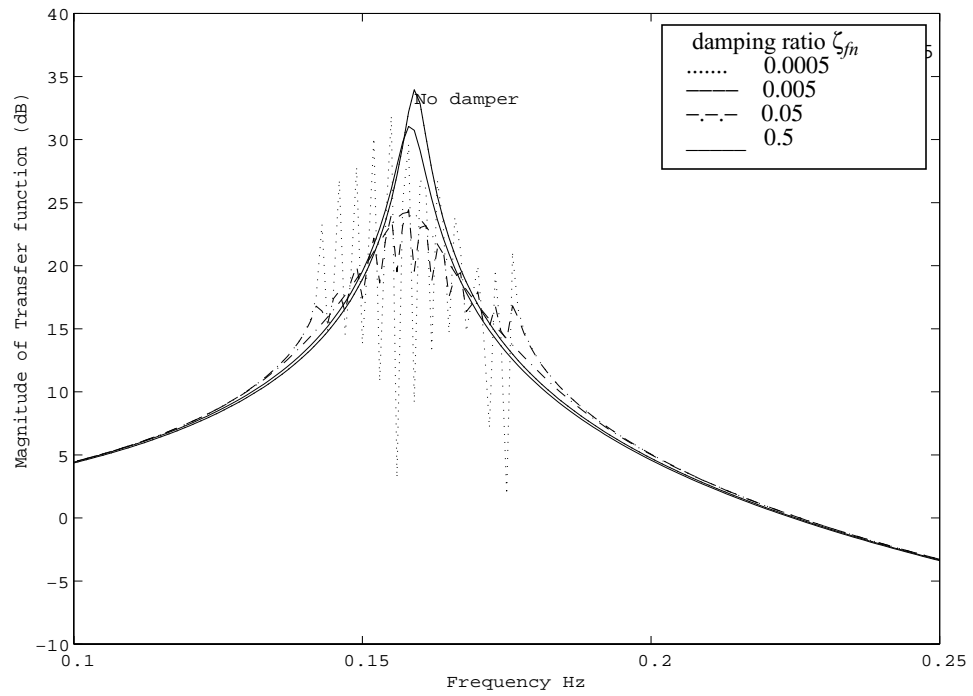


Figure 3.9 Effect of damping ratio of the dampers on the frequency response of SDOF-MTLCD system

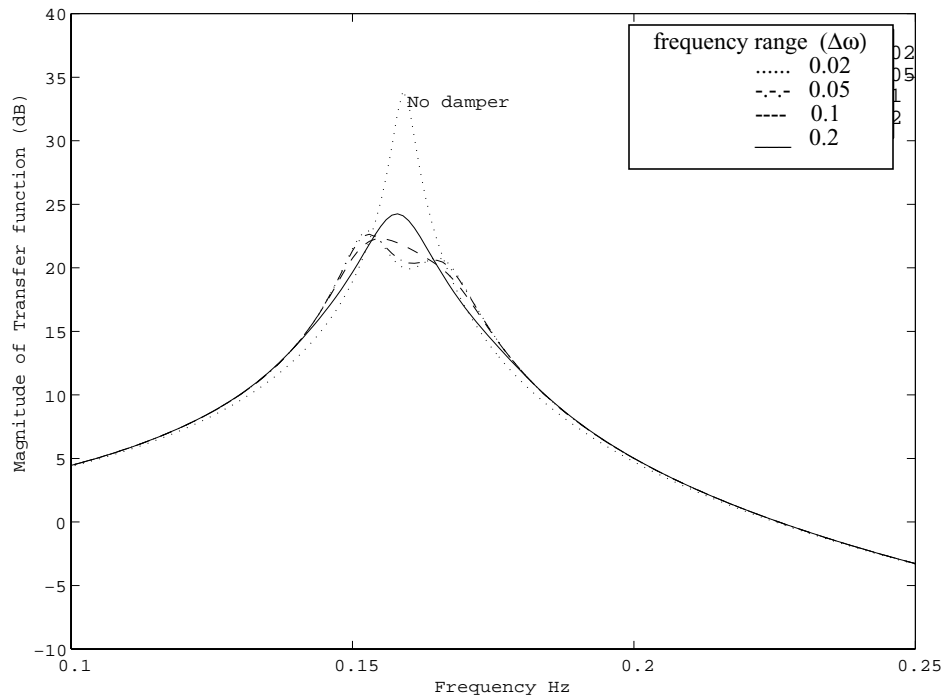


Figure 3.10 Effect of frequency range on the frequency response of SDOF-MTLCD system

TABLE 3.9 Optimum parameters for MTLCD configurations

Cases	Optimum damping ratio of each damper	Optimum frequency range	RMS displacement
No damper	-	-	12.533
N=1, STLCD	4.5%	-	7.226
N=5	1.4%	0.12	6.927
N=11	0.8%	0.145	6.878
N=21	0.6%	0.155	6.864

(These values have been computed for white noise excitation, $S_o=1$, $\omega_s=1$ rad/s, $\zeta_s=1\%$, $\mu = 1\%$)

3.5 Concluding Remarks

A method to determine the optimum absorber parameters in the case of TLCDs, using a simplified solution to the integral occurring in the estimation of the mean square response, has been presented. SDOF systems subjected to the white noise and filtered white noise excitations utilizing first and second order filters have been analyzed, and the optimum absorber parameters for TLCDs have been determined numerically based on the

minimization of the RMS displacement of the primary system. This work can be extended to MDOF systems for which a state space approach can be used and the response covariance matrix in the case of white noise can be obtained by solving the Lyapunov equation. In the case of FWN excitations, the procedure remains the same except that the primary system equations are augmented with the FWN equations.

Explicit expressions for optimal parameters are only feasible for a simple undamped primary system subjected to white noise. As the systems and forcing functions become more complex, numerical solutions are needed to evaluate the optimal parameters.

It has been seen that for lightly damped systems, the optimal damping coefficient of the absorber does not depend on the damping coefficient of the primary system when the excitation is purely white noise. However, for the first and second order FWN cases, it is affected by the primary system damping. This suggests that the damping in the primary system plays a role in determining the optimum damping coefficient of the TLCD. Although the undamped case may yield an approximate value of the optimal parameters, the primary system damping and knowledge of the excitation must be included for accurate estimates.

Optimal absorber parameters have been determined in the case of multiple TLCDs. These parameters include the number of TLCDs, the frequency range and the damping ratio of each damper. It is seen that there is an upper limit on the number of TLCDs, beyond which additional TLCDs in the MTLCD configuration do not enhance the performance. MTLCDs are more robust as compared to an STLCD and the smaller value of the optimal damping makes them more attractive for liquid dampers which have a limited range of damping. The small size of individual TLCDs in a MTLCD configuration offers convenient portability and ease of installation at different locations.